

# Heat Exchangers Modelling and Calibration for Complete ECS Architectures Simulations

*Nicolás Ablanque\*, Santiago Torras\*, Carles Oliet\*, and Joaquim Rigola\**

*\* Universitat Politècnica de Catalunya - Barcelona Tech (UPC), Heat and Mass Transfer Technological Center (CTTC)  
Terrassa, Barcelona, Spain*

## Abstract

The aeronautical industry is currently designing new Environmental Control System (ECS) architectures based on the More Electrical Aircraft (MEA) concept in order to improve the energy consumption efficiency inside commercial airplanes. The support of appropriate simulation tools is critical for this task. Within the ECS thermal perimeter, heat exchangers are arguably the most challenging components to model from the numerical and phenomenological point of views. The present work details a heat exchanger model that has been developed to fit the requirements for simulations at the architecture level: fast resolution, good accuracy and numerical robustness.

## 1. Introduction

The interest of the European aeronautical industry in the development of more efficient and environmentally friendly aircrafts is at the core of the CleanSky2 European research program. Among the most promising actions to reduce the aircraft carbon dioxide footprint, the implementation of the More Electrical Aircraft (MEA) concept stands out. This approach considers a significant reduction - or complete elimination - of bleed air from the engines in order to enhance the aircraft overall energy efficiency. The aim is to fulfil the aircraft energy demands in form of electricity generated by the engines and to free them from producing compressed air for secondary needs such as the Environmental Control System (ECS). In this sense, novel electrical Environmental Control Systems (e-ECS) based on more complex interactions with the electrical system are necessary. The e-ECS optimal design and efficient operation are critical to attain the expected global efficiency improvements as it is the largest energy consumer in large aircrafts after propulsion. The analysis of an e-ECS based on numerical simulations is particularly complex due to the large number of sub-systems involved and the different physics involved, namely, thermal, electrical, pneumatic and mechanical.

Heat exchangers are arguably the most challenging components to model within the thermal perimeter of novel aircraft e-ECSs based on the MEA approach. In particular, besides the air-to-air heat exchangers included in the traditional Air Cycle Machine (ACM), the new e-ECS systems can include additional cooling units such as Vapour Compression Systems (VCSs) which contain both condensers and evaporators. These latter heat exchangers are very complex from the phenomena point of view [1] (e.g. multi-phase characteristics, evaporation and condensation). They also face several numerical difficulties for being located within a closed refrigeration loop and being used as linking components between thermal sub-systems. The appropriate modelling of such heat exchangers must address all these challenges and possess three main characteristics: very low CPU time consumption (the ECS architecture is very large and complex so that all components must have this characteristic to prevent solver bottlenecks from happening), high numerical robustness (to address all possible operation conditions and numerical processes such as initialization or fast transients), and good accuracy (to provide useful predictions).

Two different physics-based approaches have been commonly considered for modelling the fluid flow throughout heat exchangers: the fixed volume (FV) method [2] and the moving boundary method (MB) [3]. In the FV method the flow domain discretization consists of an arbitrary number of equally sized and relatively small control volumes while the discretization of the MB method consists of only three dynamically resizable control volumes which correspond to each refrigerant phase, namely, vapor, two-phase, and liquid. The MB method can be upgraded into the switching moving boundary method (SMB) which includes the capacity to activate or deactivate any of the three aforementioned control volumes [4]. A small number of studies focused on comparing the performance of these two

methods have been reported in the open literature [6-8] such as Bendapudi et al. (2008), Rasmussen and Shenoy (2012) and Pangborn et al. (2015). Although authors report little differences in terms of accuracy between the two methods, the SMB has proven to require lower CPU time consumption while the FV has proven to be more robust, more detailed, and easier to implement.

The present work is an attempt to develop a physics-based method to integrate into the e-ECS simulations, easy to implement, fast as the SMB method, and numerically robust as the FV method. The fluid flow model developed herein has been inspired in the SMB approach as three differentiated zones are considered to account for the three possible refrigerant states but considering several simplifying assumptions and hypotheses such as steady-state calculations (the refrigerant flow is calculated from its inlet state in a sequential manner to determine the distribution of phase zones). The complete heat exchanger model combines the aforementioned steady-state approach used for both fluid flows with a transient approach used for the solid parts. This approach offers a good balance between time consumption and physical representativeness. The main features of the heat exchanger numerical model, its numerical robustness assessment, and its calibration procedure are presented in this work. The model has been developed using the Modelica language due to its advantageous characteristics for solving large complex multi-physics simulations.

## 2. Heat exchanger model

The heat exchanger model global structure, the mathematical formulation of its constitutive sub-components, and the main resolution process details are presented in this section.

### 2.1 Structure

The e-ECS thermal perimeter include several types of heat exchangers in terms of geometries, working fluids (liquids, gases, two-phase refrigerants), and phenomenological purposes such as condensation or evaporation. The heat exchanger model structure that has been implemented within this work is focused on addressing all these considerations in a flexible way. The model structure includes three main sub-components which can be easily replaced according to the specific heat exchanger characteristics. There are two sub-components to calculate the fluid flows (one for each participating fluid) and one sub-component to calculate the solid part. Figure 1 shows the model structure layout for a particular condenser that will be considered as the reference case throughout the whole document. This condenser is located inside the VCS and exchanges heat between the refrigerant and the ram air.

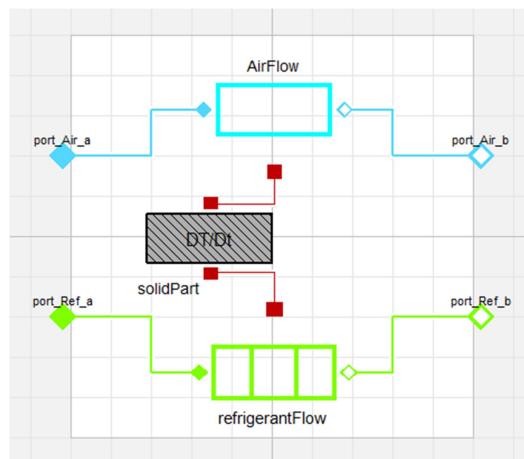


Figure 1: Model structure of studied refrigerant vs. ram air condenser.

### 2.2 Sub-components

#### Single-phase flows

The calculation of single-phase flows is based on a steady-state approach. The pressure loss is calculated based on a traditional approach where the mass flow rate is proportional to the pressure drop  $\dot{m} = K(\Delta P)^\alpha$  (the coefficients  $K$  and  $\alpha$  are previously determined from reference data). The energy conservation equation is applied between the fluid

and the solid interface and is calculated considering a single zone. The method implemented is based on an  $\varepsilon$ -NTU approach in order to optimize the calculation speed and also to prevent the involved temperatures from reaching unreal values. The sensible heat between the fluid and the solid is calculated from their temperatures:

$$\dot{Q}_{fluid} = \dot{Q}_s = \varepsilon C (T_{solid} - T_{fluid,in}) \quad (1)$$

In the case of moist air, the latent heat is also considered and the total heat transferred by the fluid is derived from both its sensible and latent terms:

$$\dot{Q}_l = \dot{m}_{da} \Delta h_{fg} (W_{out} - W_{in}) \quad (2)$$

$$\dot{Q}_{fluid} = \dot{Q}_s + \dot{Q}_l \quad (3)$$

### Two-phase flows

The calculation of two-phase flows is also based on a steady-state approach. In this case the flow model must deal with complicated phenomena as phase change occurs during evaporation or condensation processes. The method implemented in the model distinguishes three different zones, namely, gas, two-phase and liquid. Each of these zones can be active or not depending on the six different possible operating modes. The flow discretization and the corresponding operating modes of the studied condenser are detailed in Figure 2 (a similar approach is considered for evaporation cases).

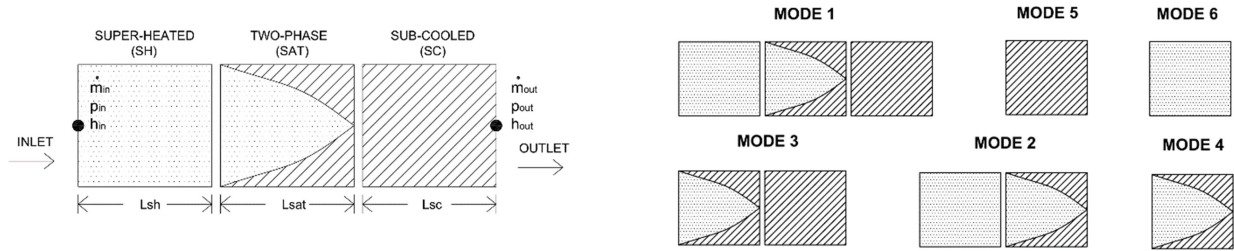


Figure 2: Two-phase flows: domain discretization (left) and operating modes (right).

The pressure drop is considered throughout the whole flow domain and it is calculated from the same approach used for single-phase flows but in this case the coefficients  $K$  and  $\alpha$  are calculated from a performance map (generated with reference data) that considers the influence of the inlet pressure, the operating mode and the mean quality value (only for operating modes including the two-phase zone). The energy conservation equation is applied between the fluid and the solid interface. The mean pressure value derived from the pressure drop calculations is used to approximate the corresponding liquid and gas specific enthalpy saturation values.

The resolution is conducted isobarically from both the inlet specific enthalpy and the mass flow rate values in a sequential manner. For instance, if the inlet condition of a condenser is super-heated, the first zone to be calculated corresponds to the super-heated zone. If the predicted heat surpasses the maximum heat allowed for this particular zone (i.e. heat obtained from the inlet condition and the vapor saturation limit) the corresponding heat for this zone will be that maximum one and the calculation will proceed with the following zone (i.e. two-phase zone). For single-phase zones the heat is calculated as explained in the previous section to prevent unreal predictions while the heat corresponding to two-phase zones is calculated from a standard approach:

$$\dot{Q}_{fluid} = \alpha (T_{solid} - T_{fluid,sat}) A \quad (4)$$

The process keeps going until the heat does not surpass the corresponding maximum heat of the zone being calculated.

### Solid parts

The solid part represents the thermal link between the two flows and considers a unique temperature. Its calculation includes the dynamic terms:

$$MC_p(dT/dt) - \dot{Q}_{fluid1} - \dot{Q}_{fluid2} = 0 \quad (5)$$

### 2.3 Resolution

The complete resolution is carried out by means of the default differential/algebraic system solver of Dymola. The heat exchanger model combines the steady-state approach used for both flows with the dynamic approach considered for the solid part. Therefore, the model overall thermal response is dynamic as it includes not only the thermal inertia of the solid part but also the possibility to apply artificial relaxations to the energy conservation equations of both fluid flows (i.e. to further overcome the negative impact of the absence of dynamic terms). The pressure drop equation is not only used to calculate the mass flow rate but also to approximate the phase saturation limits needed for the energy conservation equation.

## 3. Numerical assessment

The present section addresses the model numerical characteristics in terms of CPU time consumption and robustness. Heat exchanger models must satisfy many numerical requirements for their successful use when simulating complex thermal architectures where a large number of components and systems are interacting and appropriately low simulation time is required for real time control purposes or massive amount of steady-state cases for design purposes. Heat exchangers must be able to provide robust simulations at unexpected thermal characteristics that could occur during particular transients, numerical iterations, and off-design operation conditions. The following list summarizes the expected capacities of the model:

- The numerical simulation must be robust to any setup parameter used such as number of time intervals. No numerical tuning should be necessary to run different cases.
- Null mass flow rate and reversed flow conditions must be handled by both fluids of the heat exchanger.
- The heat exchanger must handle unexpected changes on the main heat flow direction due to eventual temperature variations of the participating fluids.
- The heat exchanger model must be sturdy to any possible boundary condition type (e.g. pressure, mass flow rate) and signal type (e.g. step, ramp, and sines).
- The model CPU time consumption must be relatively low to prevent bottlenecks from happening at both system and architecture levels.

The heat exchanger model developed has been subjected to a comprehensive set of tests to assess its robustness and evaluate its time response. In the following sub-sections these tests are briefly described (for the particular case of the aforementioned refrigerant-to-air condenser) and the global performance characteristics are presented. Most of the variables are presented in a normalized way derived from reference values due to confidentiality reasons:

$$\theta_{norm} = \theta/\theta_{ref} \quad (6)$$

### 3.1 Initialization

The initialization process of dynamic solvers often presents numerical challenges due to the unknown information of the previous time step and the difficulty to define appropriate initial values. The initialization process of the present model has been tested by initializing the model considering a complete set of cases covering the complete range of input conditions and their possible combinations. The parameters ranges used for this test are described in Table 1.

Table 1: Ranges applied for initialization test.

Parameter	Values
Normalized air mass flow rate	0.4/1.0/1.8
Normalized refrigerant mass flow rate	0.5/1.0/1.5
Normalized refrigerant pressure	0.5/1.0
Refrigerant inlet enthalpy	3 values (to ensure inlet conditions for each phase zone)
Air inlet temperatures	4 values (based on the saturation temperature)

### 3.2 Mode switching

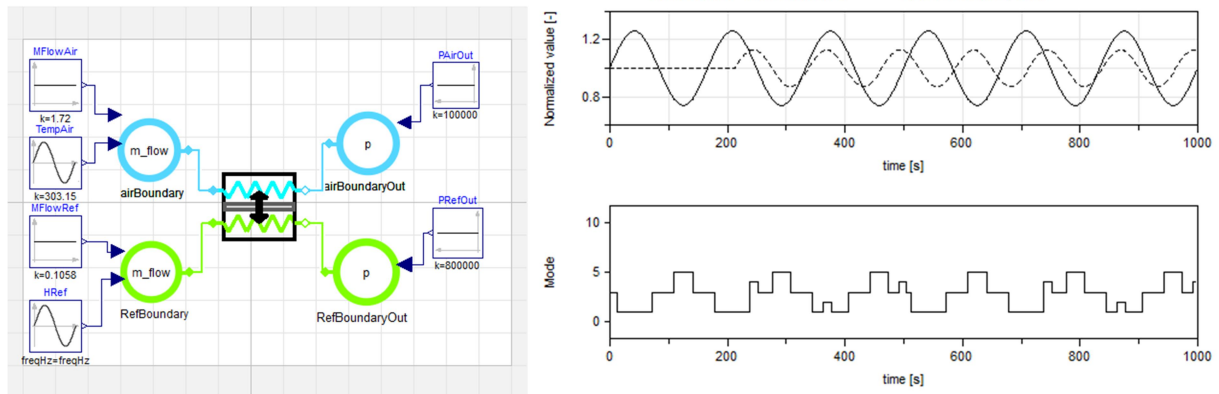


Figure 3: Mode switching: test scheme (left) and illustrative results (right).

The two-phase flow method considers different operating modes as shown in Figure 2. The model must ensure its robustness when switching from one mode to another during simulations. Therefore, the model has been tested during such transitions by modifying the values of different input variables during the simulation (e.g. air inlet temperature and refrigerant inlet specific enthalpy). The test scheme and some illustrative results are presented in Figure 3.

### 3.3 Input signals

Another important numerical consideration for the model is to ensure its appropriate transient response when experiencing changes on the boundary values. This aspect is crucial for components used within systems as they are linked to other components, and therefore, exposed to changing values during transient simulations and solver iterations. In order to ensure the model robustness in this particular sense, a complete set of tests considering two different type of signals (ramps and sines) has been conducted. The ramp and sine test schemes and their corresponding illustrative examples are shown in Figure 4 and Figure 5, respectively.

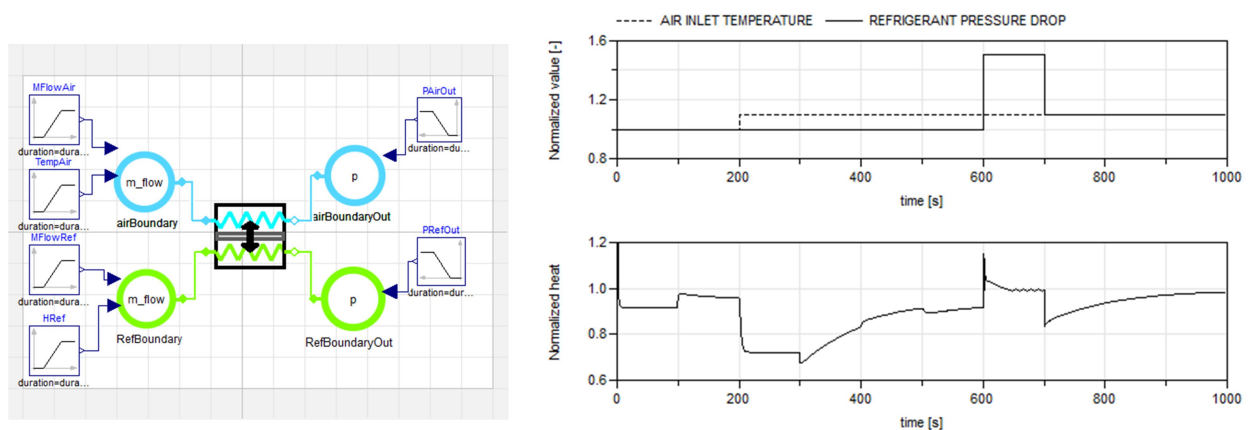


Figure 4: Ramp signal: test scheme (left) and illustrative results (right).

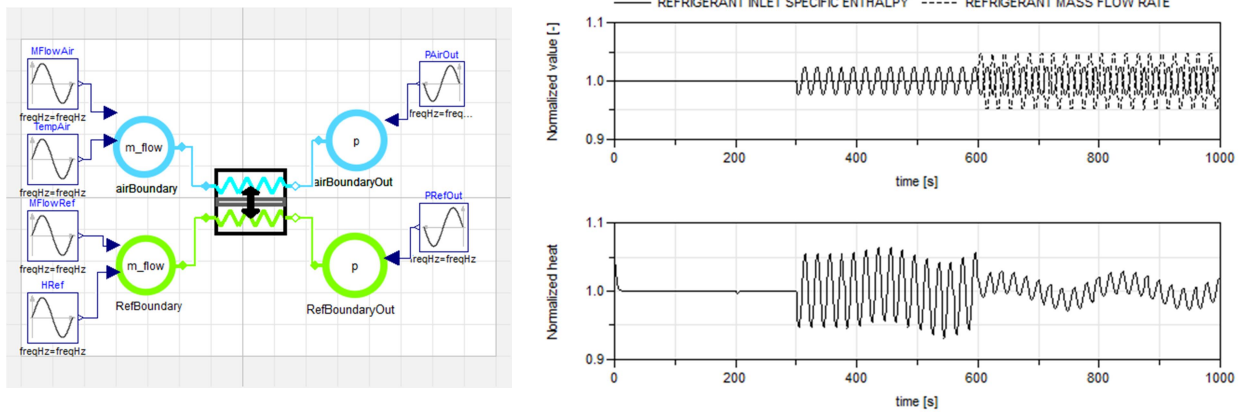


Figure 5: Sine signal: test scheme (left) and illustrative results (right).

### 3.4 Reversed heat

The model must address changes of the heat direction that could occur at some specific system operation conditions or solver iterating process. For instance, in the studied condenser the heat could eventually flow from the secondary fluid toward the refrigerant. To ensure the model robustness a set of tests where the heat direction is forced to change has been implemented. The runs used to evaluate the reversed heat capacity were conducted by modifying the inlet temperature of the air by means of a ramp signal up to a value higher than the refrigerant inlet temperature so that the condenser heat flow direction is changed. The test scheme and a particular illustrative result are shown in Figure 6.

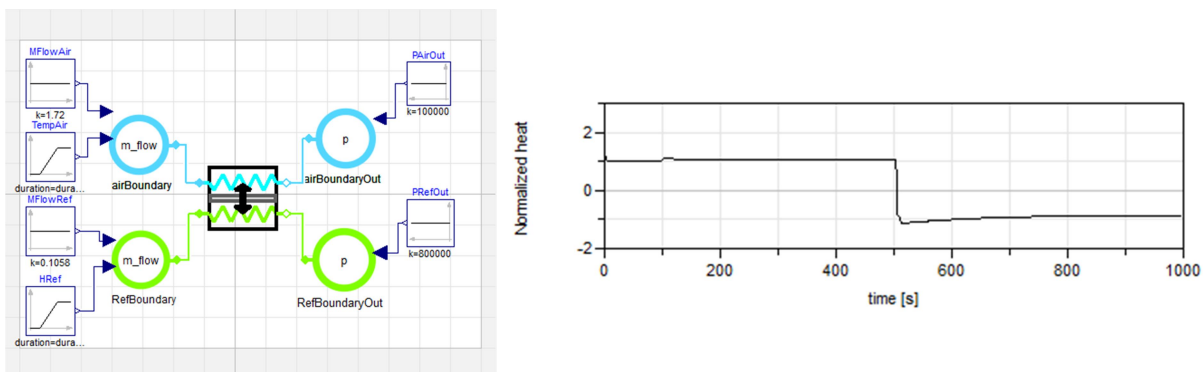


Figure 6: Reversed heat: test scheme (left) and illustrative results (right).

### 3.5 Reversed and null mass flow rate

The aim of this final test is to address the model capacity to handle reversed and null mass flow rates on both fluids. This aspect is crucial as these particular conditions could happen during the system start-up, shut-down or any other eventuality. Each particular run consists of a transient case where the refrigerant is operating at a particular mode and one of the fluids experiences both flow direction changes and null mass flow rate at different moments. The test scheme and some illustrative results are presented in Figure 7 (in this particular case flow direction changes are applied to the refrigerant flow).

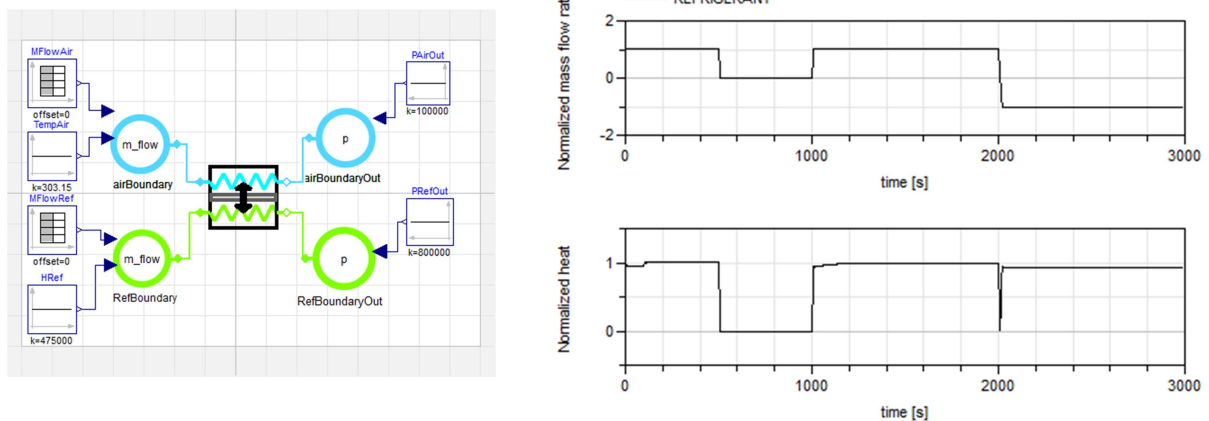


Figure 7: Reversed and null mass flow rate: test scheme (left) and illustrative results (right).

### 3.6 Global numerical assessment

The full set of tests described in the previous sections consisted of 648 cases in total. For each particular test, different numerical setups were considered (number of time intervals) as well as two different boundary condition configurations (pressure vs. pressure and pressure vs. mass flow rate) in order to address the non-causality nature of Modelica (see Figure 8).



Figure 8: Tests boundary configurations considered.

The robustness of the model has been evaluated based on the number of failed runs. For the particular condenser case that has been studied the results are summarized in Table 2. It can be seen that all the cases tested converge to a solution without any particular issue (only one case is considered as a failure as it largely surpasses the expected CPU time). The mean CPU calculation time for all the tests is significantly low taking into account both the simulation time and the demanding transient characteristics considered for tests. The percentage of run failures is relatively low compared to the number of cases tested, therefore, a good global numerical robustness has been achieved for the condenser model. The characteristics of the processor used are: Intel(R) Core(TM) i5-2450M CPU @ 2.60GHz 2.60 GHz.

Table 2: Tests numerical assessment: summarized results.

Test	Cases	Stop time [s]	Intervals	Mean CPU time [s]	Failures
Initialization	432	2000	2000	0.24*	1*
Switching	36	1000	500/1000/2000	0.65	0
Ramps	36	1000	500/1000/2000	0.46	0
Sines	36	1000	500/1000/2000	2.97	0
Heat reversed	36	1000	500/1000/2000	0.26	0
Flow (null/reversed)	72	3000	1500/3000/6000	0.82	0
<b>Total</b>	<b>648</b>				<b>1</b>

\*Mean CPU time calculated without including the failed case

## 4. Calibration assessment

The developed physical model has been based on several simplifying assumptions so that specific calibration procedures have been added to the model for accuracy improvement. Both pressure drop and heat transfer calculations have been calibrated with reference data obtained from a more advanced detailed heat transfer model.

### 4.1 Pressure drop

The pressure drop equation used for the model is based on the basic expression as it has proven to be robust in terms of numerical stability.

$$\dot{m} = K(\Delta P)^\alpha \quad (7)$$

The coefficients  $K$  and  $\alpha$  are derived from reference data and depend on several parameters such as the inlet pressure, the operation mode, and the mean two-phase zone quality (the latter parameter is only considered when the two-phase zone is present). Figure 9 shows an example of curve fitting for the studied condenser working at mode 4 (pure two-phase flow, see Figure 2) and for a particular inlet pressure value.

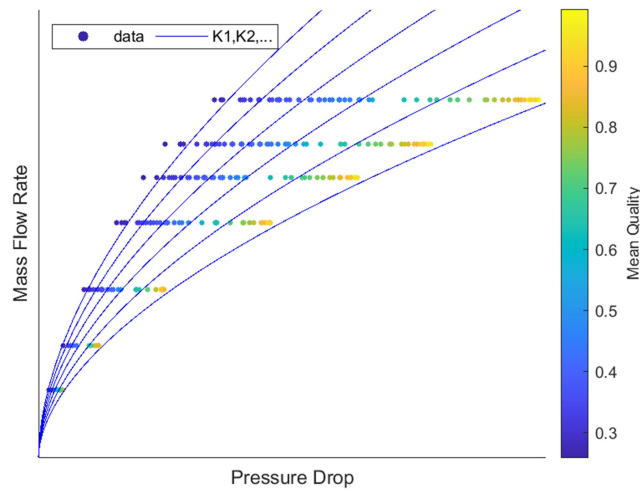


Figure 9: Example of curve fitting from the pressure drop vs. mass flow rate reference information (illustrative case for operation mode 4).

The model pressure drop prediction accuracy has been evaluated based on the Prediction Error (PE) parameter which characterizes the difference between the model predicted value and the reference value of a particular variable. The local PE is a percentage value and is evaluated as follows:

$$PE = \frac{|\theta_{model} - \theta_{ref}|}{\theta_{ref}} \times 100 \quad (8)$$

To assess the accuracy regarding the whole data, an averaged PE is used: The Mean Prediction Error (MPE) which is defined as follows:

$$MPE = \frac{1}{N} \sum_{i=1}^{i=N} PE_i \quad (9)$$

A set of 4764 reference simulations has been used to compare the model accuracy for the pressure drop calculation. The mean prediction error obtained was 9.40% for the 100% of the data points and 4.65% for 75% of the data points.

## 4.2 Heat transfer

The heat exchanger model developed must be fed with values for the empirical heat transfer coefficients used to calculate the heat transfer for each fluid flow. In the case of single-phase flows (e.g. air and liquid) a unique heat transfer coefficient value is needed, while for the case of multi-phase flows (e.g. refrigerant) three different coefficient values are needed, one for each specific phase zone, namely, liquid, two-phase, and vapor. The model allows different ways to determine these heat transfer coefficients: as constant values, derived from performance maps, or alternatively, calculated from more specific correlations. The particular correlations used in the condenser model cannot be disclosed.

In addition, the heat transfer calculation includes a global correction performance map that is obtained from the reference data. The aim of this map is to provide a parameter that corrects the total heat flow predicted by the model depending on several parameters such as the condenser operating mode, the mass fluxes of the participating fluids, and the mean quality of the two-phase zone if it exists. The comparison between reference data and model predictions in terms of total heat exchanged is presented in Figure 10 for both the model without the global correction and the model with the global correction (the actual heat values are not plotted due to confidentiality restrictions).

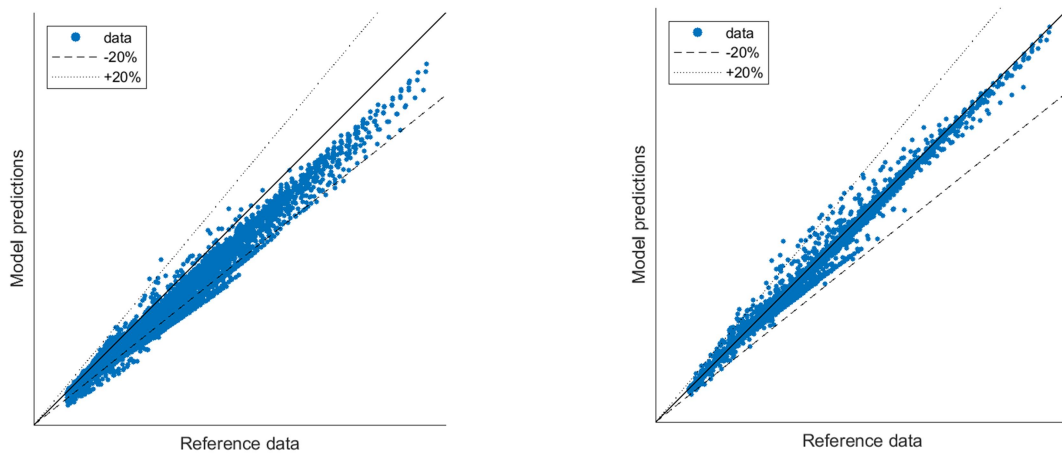


Figure 10: Model heat transfer accuracy assessment: without global calibration (left) with global calibration (right).

From Figure 10 it is observed that a generalized under-prediction of data occurs when no correction is applied. It is also noticed how this particular trend is significantly mitigated as the correction information is used. In order to assess the model accuracy more precisely the MPE has been calculated for both cases. The results are detailed in Table 3. A set of 4764 reference simulations has been used to compare the model accuracy in terms of heat transfer. The mean prediction error obtained for the whole data was 10.01% and 2.48% for the model without and with the correcting performance map, respectively. It is clear how the results agreement has significantly improved with the use of the correction. It has also observed how the accuracy increases as the most divergent cases are removed (e.g. from 100% to 75% of the data).

Table 3: Model heat transfer accuracy assessment in terms of MPE

Data [%]	Model (not calibrated)			Model (calibrated)		
	MPE [%]	MaxPE [%]	$\sigma$	MPE [%]	MaxPE [%]	$\sigma$
100	10.01	44.17	7.11	2.48	42.09	3.77
98	9.55	27.44	6.38	2.12	15.51	2.68
95	9.04	23.39	5.79	1.78	10.46	1.92
90	8.34	20.08	5.10	1.43	5.85	1.20
85	7.73	17.70	4.55	1.23	4.06	0.88
75	6.69	13.68	3.74	0.99	2.28	0.61

## 5. Conclusions

A heat exchanger model based on the combination of steady-state and transient calculations has been developed to be used within the thermal perimeter of large e-ECS architectures. The model has been developed to appropriately achieve the three main characteristics required for its use on such complex and large architectures:

- Low CPU time consumption. The simplified method implemented allows to conduct fast calculations and at the same time to consider three different phase zones for the refrigerant fluid to better represent the phenomenology in such cases. Transient and steady-state simulations have been conducted in just a fraction of a second while very demanding transient simulations with multiple sine-type signals have converged in just very few seconds (see Table 2). The real time factor for all simulations was very low (e.g. 0.00012 for the initialization tests).
- High numerical robustness. Heat exchangers are the most critical components of the thermal perimeter due to their complex phenomena, their thermal linking role between systems, and the wide variety of input data combinations that they can be subjected to. The model has been comprehensively tested to ensure its numerical robustness at all levels. It has proven to be sturdy regarding many different numerical aspects (initialization, numerical setup, boundaries configuration, input signals type) and many off-design operation conditions (reversed heat flow direction, changes on fluid flows directions, and null mass flow rates). These characteristics are crucial to tackle specific transients (e.g. start-ups, shut-downs, malfunctions, etc...) but also unpredictable iteration conditions during solver resolution.
- Good accuracy. The developed heat model is based on a simplified physical approach which allows a more confident prediction of untested conditions. The model is fed with empirical maps to calculate both the pressure drop and the heat exchanger coefficients but also with a correction map derived from a calibration procedure based on reference data. The latter correction map has proven to significantly increase the model accuracy level from a MPE of 10.01% to a MPE of 2.48% in terms of heat transfer. A more accurate model will not represent major improvements for simulations at the architecture level.

## Nomenclature

A	Heat transfer area	$m^2$
C	Heat capacity rate	$W K^{-1}$
$C_p$	Specific heat capacity	$J kg^{-1} K^{-1}$
h	Specific enthalpy	$kJ kg^{-1}$
L	Length	m
$\dot{m}$	Mass flow rate	$kg s^{-1}$
M	Mass	kg
P	Pressure	Pa
$\dot{Q}$	Heat flow	W
RTF	Real Time Factor	-
t	Time	s
T	Temperature	K
W	Humidity ratio	$kg_v kg_{da}^{-1}$

### Greek symbols

$\Delta h_{fg}$	Enthalpy of vaporization	$J kg^{-1}$
$\varepsilon$	Effectiveness	-
$\theta$	Variable	-
$\sigma$	Standard deviation	-

### Subscripts

da	Dry air
fluid	Fluid
in	Inlet
l	Latent
norm	Normalized
out	Outlet

ref	Reference
s	Sensible
solid	Solid
v	Vapor

## References

- [1] Rasmussen, B.P. 2012. Dynamic modelling for vapour compression systems – part I: literature review. *HVACR Res.*, 18(5), pp. 934-955.
- [2] Morales-Ruiz, S., Rigola, J., Pérez-Segarra, C.D., and García-Valladares, O. 2009. Numerical Analysis of two-phase flow in condensers and evaporators with special emphasis on single-phase/two-phase transition zones. *Applied Thermal Engineering*, 29(5-6), pp. 1032-1042.
- [3] Jensen, J.M., and Tummescheit, H. 2002. Moving boundary models for dynamic simulations of two-phase flows. *In Modelica 2002 Proceedings*. Modelica Association, pp. 234-244.
- [4] Qiao, H., Laughman, C.R., Aute, V., and Radermacher, R. 2016. An advanced switching moving boundary heat exchanger model with pressure drop. *International Journal of Refrigeration*, 65, pp. 154-171.
- [5] Rasmussen, B.P., and Shenoy, B. 2012. Dynamic modelling for vapour compression systems – part II: simulation tutorial. *HVACR Res.*, 18(5), pp. 956-973.
- [6] Bendapudi, S., Braun, J.E., and Groll, E.A. 2008. A comparison of moving-boundary and finite volume formulations for transients in centrifugal chillers. *International Journal of Refrigeration*, 31(8), pp. 1437-1452.
- [7] Pangborn, H., Alleyne, A.G., and Wu, N. 2015. A comparison between finite volume and switching moving boundary approaches for dynamic vapor compression system modeling. *International Journal of Refrigeration*, 53, pp. 101-114.

## Acknowledgement

This project has received funding from the Clean Sky 2 Joint undertaking (JU) under grant agreement No 886533. The JU receives support from the European Union's Horizon 2020 research and innovation programme and the Clean Sky 2 JU members other than the Union.



Carles Oliet, as a Serra Hünter lecturer, acknowledges the Catalan Government for the support through this Program.

**Disclaimer:** The contents presented in this article reflect only the author's point of view: the authors and Clean Sky 2 JU are not responsible for any use that may be made of the information it contains.